

## Vibrational Spectral Investigations, NLO and Homo LUMO Analysis of 4-Chloro-2, 6-Dibromoaniline

M.Rajasekaran<sup>1</sup>, P.Kumaresan<sup>2</sup> and K.Sambathkumar<sup>3,\*</sup>

<sup>1</sup>Bharathiyar University, Coimbatore, Tamilnadu. 641046. India.

<sup>2</sup>Department of Physics, Thiru.A.Govindasamy Govt Arts College, Tindivanam 604002. Tamilnadu. India.

<sup>3</sup>Department of Physics, A.A.Govt. Arts College, Villupuram-605602. Tamilnadu. India.

### ARTICLE INFO

#### Article history:

Received: 31 December 2015;

Received in revised form:

10 March 2016;

Accepted: 15 March 2016;

#### Keywords

FTIR,

FT-Raman,

CDBA,

HOMO,

LUMO,

TED.

### ABSTRACT

The solid phase FTIR and FT-Raman spectra of 4-chloro-2, 6-dibromoaniline (CDBA) have been recorded in the region 4000-400 cm<sup>-1</sup> and 3500-100 cm<sup>-1</sup>, respectively. The spectra were interpreted with the aid of normal coordinate analysis following a full structure optimization and force field calculation based on the density functional theory (DFT) using the standard HF/6-31+G(d,p) and B3LYP/6-31+G(d,p) methods and basis set combination. A close agreement between the observed and calculated frequencies by refinement of the scale factor. The values of electric dipole moment ( $\mu$ ) and First-order hyperpolarizability ( $\beta$ ) of the compound were computed using ab-initio quantum mechanical calculations. The calculation results also show that the PFA molecule might have microscopic nonlinear optical (NLO) behavior with non-zero values. HOMO and LUMO energy gap explains the eventual charge transfer interaction taking place within the molecule.

© 2016 Elixir all rights reserved.

### Introduction

Aniline and its derivatives have been widely used as starting materials in a vast amount of chemicals, pharmaceuticals, dyes, electro-optical and many other industrial processes [1-4]. The conducting polymer of aniline, namely, poly aniline is used in microelectronic devices as diodes and transistors [5-8]. Particularly, aniline and its derivatives are used in the production of dyes, pesticides and antioxidants. Consideration of these factors leads to undertake the detailed spectral investigation of 4-chloro-2, 6-dibromoaniline (CDBA). The aim of this work is to carry out an experimental and theoretical study on these compounds with the methods of quantum chemistry, in order to have a better understanding of its vibrational properties. However, for a proper understanding of IR and Raman spectra, reliable assignments of all vibrational bands are essential. Recently, computational methods based on density functional theory are being widely used. These methods predict a relatively accurate molecular structure and vibrational spectra with moderate computational effort. In particular, for polyatomic molecules, the DFT methods lead to the prediction of more accurate molecular structure and vibrational frequencies than the conventional *ab initio* restricted Hartree-Fock (HF) and Moller-Plesset second order perturbation theory (MP2) calculations [9-12]. To the best of our knowledge, there is no theoretical calculation to understand the structure and the fundamental vibrational frequencies of CDBA and PFA. This study is made to present a full description of the vibrational spectra of the title compounds, using *ab initio* HF and DFT (B3LYP) with 6-31+G(d,p) to obtain the geometries, vibrational frequencies, IR intensities and Raman activities. The atomic charges, distribution of electron density (ED) in various bonding and antibonding orbitals and stabilisation

energies,  $E^{(2)}$  have been calculated by natural bond orbital (NBO) analysis.

### Experimental Details

The spectroscopically pure grade sample of CDBA are obtained from Lancsaster Chemical Company, UK and used as such for the spectral measurements.

The FTIR spectra of CDBA is recorded in the region 4000 - 400 cm<sup>-1</sup> at a resolution of  $\pm 1$  cm<sup>-1</sup> using BRUKER IFS 66V model FTIR spectrometer equipped with an MCT detector, a KBr beam splitter and global arc source. The FT-Raman spectra of CDBA is recorded using 1064 nm line of Nd:YAG laser as excitation wavelength in Stokes region (3500-100 cm<sup>-1</sup>) on a BRUKER IFS-66 V model interferometer equipped with FRA-106 FT-Raman accessories operating at 200 mW power. The calibrated wave numbers are expected to be accurate within  $\pm 1$  cm<sup>-1</sup>.

### Computational Details

In order to provide information with regard to the structural characteristics and the normal vibrational mode of CDBA, the Hartree-Fock and DFT-B3LYP correlation functional calculations have been carried out. The entire calculations are performed using the GAUSSIAN 09W software package [13]. Initially, the HF level calculations, adopting the 6-31+G(d,p) basis set are carried out and then the DFT employing the Becke 3LYP keyword, which invokes Becke's three-parameter hybrid method has been computed using the correlation function of Lee *et al.* [14], implemented with the 6-31+G(d,p) basis set. All the parameters are allowed to relax and all the calculations converge to an optimized geometry which corresponds to a true minimum, as revealed by the lack of imaginary values in the wave number calculations. The Cartesian representation of the theoretical force constants has been computed at the fully optimized

geometry. Transformation of force field, the subsequent normal co-ordinate analysis including the least square refinement of the scale factors and calculations of Total energy (TED) are done on a PC with the MOLVIB program (version V7.0 – G77) and written by Sundius [15-17]. The symmetry of the mode is also helpful in making vibrational assignments by combining results of GAUSSVIEW Program with symmetry consideration, vibrational frequency assignments are made with a high degree of confidence. There is always some ambiguity in defining internal coordinate. However, the defined coordinate form complete set and matches quite well with the motions observed using the GAUSSVIEW program [18]. The systematic comparison of the results from DFT theory with results of experiments has been shown that the method using B3LYP functional is the most promising in providing correct vibrational wave numbers.

#### Prediction of Raman intensities

The Raman activities ( $S_i$ ) calculated with the GAUSSIAN 09W program are subsequently converted to relative Raman intensities ( $I_i$ ) using the following relationship derived from the basic theory of Raman scattering [19-21],

$$I_i = \frac{f(v_0 - v_i)^4 S_i}{v_i \left[ 1 - \exp\left(-\frac{hc v_i}{kT}\right) \right]}$$

where  $v_0$  is the exciting frequency in  $\text{cm}^{-1}$ ,  $v_i$  the vibrational wave number of the  $i^{\text{th}}$  normal mode,  $h$ ,  $c$  and  $k$  are the fundamental constants and  $f$  is a suitably chosen common normalization factor for all the peak intensities.

#### Results and Discussion

##### Molecular geometry

The optimized molecular structure of CDDBA is shown in Fig. 1, respectively.

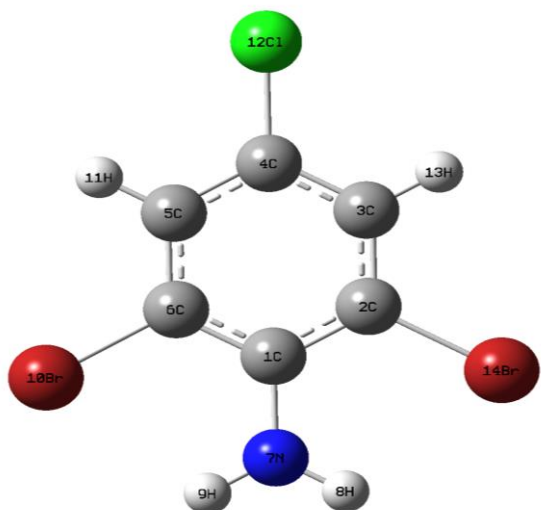


**Fig 1. Molecular structure of 4-chloro-2,6-dibromoaniline**

The optimization geometrical parameters of CDDBA obtained by the HF, DFT/ B3LYP with 6-31+G(d,p) as basis set are listed in Table 1, respectively. The structural data provided in Table 1 indicate that various bond lengths are found to be almost same at HF/6-31+G(d,p) and B3LYP/6-31+G(d,p) levels. However, the B3LYP/6-31+G(d,p) level of theory, in general slightly overestimates the bond lengths but it yields bond angles in excellent agreement with the HF method. The calculated geometrical parameters are compared with X-ray diffraction results [22,23].

The calculated geometric parameters agree well with almost all values. The small deviations are probably due to the intermolecular interactions in the crystalline state of the molecule. Detailed description of vibrational modes can be given by means of normal coordinate analysis. The internal coordinates describe the position of the atoms in terms of distances, angles and dihedral angles with respect to an origin atom. The symmetry coordinates are constructed using the set of internal coordinates. In this study, the full sets of 48 standard internal coordinates (containing 12 redundancies) for CDDBA are defined as given in Table 2. From these, a non-redundant set of local symmetry coordinates are constructed by suitable linear combinations of internal coordinates following the recommendations of Fogarsi *et al.* [24] and is summarized in Table 3. The theoretically calculated DFT force fields are transformed to this later set of vibrational coordinates and used in all subsequent calculations.

Using the DFT/B3LYP with large basis set calculations, several thermodynamic properties of CDDBA have been calculated. The values obtained for zero-point vibrational energy, rotational constants, rotational temperature, thermal energy, molar capacity at constant volume, entropy and dipole moment along with the global minimum energy are presented in Table 4 for CDDBA, respectively. The difference in the values calculated by the method is only marginal. The variation in the ZPVE seems to be insignificant. The total energy and the change in the total entropy of the molecule at room temperature are also presented.

##### Vibrational Spectra

From the structural point of view the CDDBA is assumed to have  $C_s$  point group symmetry. Both the compounds 36 normal modes of vibrations are distributed among the symmetry species as

$$3N - 6 = 25 A' (\text{in-plane}) + 11 A'' (\text{out-of-plane})$$

The  $A'$  and  $A''$  species represent the in-plane and out-of-plane vibrations, respectively. The detailed vibrational assignments of fundamental modes of CDDBA along with calculated IR, Raman intensities, force constants and normal mode descriptions (characterized by TED) are reported in Table 5. The FTIR and FT-Raman spectra of CDDBA are shown in Fig.2-3.

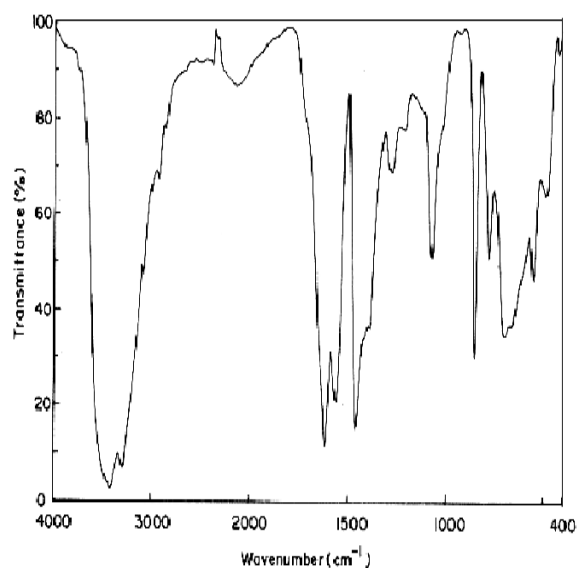


**Fig 2. FTIR spectrum of 4-chloro-2,6-dibromoaniline**

**Table 1. Optimized geometrical parameters of 4-chloro-2,6-dibromoaniline obtained by HF/6-31G+(d,p) and B3LYP/6-31+G(d,p) density functional theory calculations**

Bond length	Value (Å)			Bond angle	Value (°)		Exp	Value (°)		
	HF/6-31G+(d,p)	B3LYP/6-31G+(d,p)	Exp		HF/6-31G+(d,p)	B3LYP/6-31G+(d,p)		Dihedral angle	HF/6-31G+(d,p)	B3LYP/6-31G+(d,p)
C1-C2	1.3937	1.4075	1.404(6)	C1-C2-C3	122.1163	122.7406	119	C6-C1-C2-C3	-0.0402	0.2398
C2-C3	1.3799	1.3955	1.380(7)	C2-C3-C4	119.0479	118.8985	117	C6-C1-C2-Br10	179.5686	-179.3282
C3-C4	1.3879	1.3904	1.386(7)	C3-C4-C5	120.1740	120.8969		N7-C1-C2-C3	176.956	-176.8392
C4-C5	1.3797	1.3914	1.386(7)	C4-C5-C6	119.3945	118.8987		N7-C1-C2-Br10	-3.4352	3.6019
C5-C6	1.3813	1.3924	1.380(7)	C5-C6-C1	122.8812	123.7405	117	C2-C1-C6-C5	0.0403	-0.2402
C6-C1	1.3946	1.4083	1.404(6)	C6-C1-C2	116.3862	115.8293	122	C2-C1-C6-Br14	-179.5686	179.8297
C1-N7	1.4137	1.4234		C6-C1-N7	122.4523	122.0813		N7-C1-C6-C5	-179.9559	176.8297
N7-H8	1.0000	1.0178		C2-C1-N7	122.1615	122.0813		N7-C1-C6-Br14	3.4352	-3.6022
N7-H9	1.0000	1.0178		H8-N7-H9	115.2029	106.2400		C2-C1-C7-H8	23.5071	-21.8736
C2-Br14	1.8928	1.9063		C3-C4-Cl12	119.2547	119.5515		C2-C1-N7-H9	159.6518	-161.2186
C3-H13	1.0716	1.0828		C5-C4-Cl12	119.6290	119.5515		C6-C1-N7-H8	-159.6519	161.2188
C4-Cl12	1.7404	1.7565		C2-C3-H13	120.0927	120.4017		C6-C1-N7-H9	-23.5071	121.8738
C5-H11	1.0716	1.0828		C4-C3-H13	120.8595	120.6997		C1-C2-C3-C4	-0.1179	0.0255
C6-Br10	1.8928	1.9062		C4-C5-H11	120.1316	120.6996		C1-C2-C3-H11	179.8809	-179.9171
				C6-C5-H11	120.4740	120.4017		Br10-C2-C3-C4	-179.724	179.5885
				C5-C6-Br10	117.8967	118.5829		Br10-C2-C3-H11	0.2748	-0.354
				C1-C6-Br10	119.2221	118.6762		C2-C3-C4-C5	0.2744	-0.2980
				C1-C2-Br14	119.6851	118.6759		C2-C3-C4-Cl12	-179.996	179.8862
				C3-C2-Br14	117.6851	118.5831		H11-C3-C4-C5	-179.7244	179.6427
				C1-N7-H8	117.4569	117.5672		H11-C3-C4-Cl12	0.0052	-0.1713
				C1-N7-H9	117.3691	117.5681		C3-C4-C5-C6	-0.2744	0.2995
								C3-C4-C5-H13	179.7244	-179.643
								Cl12-C4-C5-C6	179.9961	-179.8865
								Cl12-C4-C5-H13	-0.0051	0.171
								C4-C5-C6-C1	0.1178	-0.0249
								C4-C5-C6-Br14	179.7239	-179.588
								H13-C5-C6-C1	-179.881	-179.9176
								H13-C5-C6-Br14	-0.2749	0.3545

For numbering of atoms refer Fig. 1.  
Ref. [29]

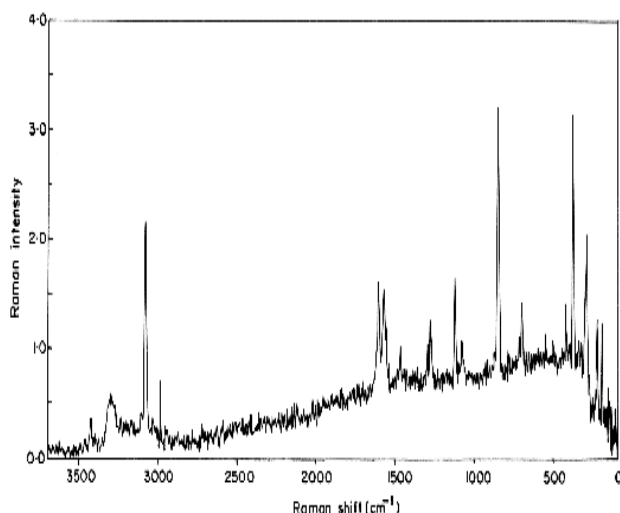


Fig 3. FT-Raman spectrum of 4-chloro-2,6-dibromoaniline

Table 2. Definition of internal coordinates of 4-chloro-2,6-dibromoaniline

No. (i)	Symbol	Type	Definition <sup>a</sup>
<b>Stretching</b>			
1 – 2	$r_i$	C–H	$C_3-H_{11}, C_5-H_{13}$
3,4	$R_i$	C–Br	$C_2-Br_{10}, C_6-Br_{14}$
5	$q_i$	C–Cl	$C_4-Cl_{12}$
6	$Q_i$	C–N	$C_1-N_7$
7 – 12	$S_i$	C–C	$C_1-C_2, C_2-C_3, C_3-C_4, C_4-C_5,$ $C_5-C_6, C_6-C_1$
13, 14	$p_i$	N–H	$N_7-H_8, N_7-H_9$
<b>In-plane bending</b>			
15 – 20	$\alpha_i$	Ring	$C_1-C_2-C_3, C_2-C_3-C_4, C_3-C_4-C_5,$ $C_4-C_5-C_6, C_5-C_6-C_1, C_6-C_1-C_2$
21 – 24	$\beta_i$	C–C–H	$C_2-C_3-H_{11}, C_4-C_5-H_{11}, C_4-C_5-H_{13},$ $C_6-C_5-H_{13}$
25 – 26	$\nu_i$	C–C–Cl	$C_3-C_4-Cl_{12}, C_5-C_4-Cl_{12}$
27, 30	$\sigma_i$	C–C–Br	$C_1-C_2-Br_{10}, C_3-C_2-Br_{10},$ $C_5-C_6-Br_{14}, C_1-C_6-Br_{14}$
31, 32	$\delta_i$	C–C–N	$C_6-C_1-N_7, C_2-C_1-N_7$
33, 34	$\epsilon_i$	C–N–H	$C_1-N_7-H_8, C_1-N_7-H_9$
35	$\pi_i$	H–N–H	$H_8-N_7-H_9$
<b>Out-of-plane bending</b>			
36, 37	$\psi_i$	C–H	$H_{11}-C_3-C_4-C_2, H_{13}-C_5-C_6-C_4$
38	$\omega_i$	C–Cl	$Cl_{12}-C_4-C_5-C_3$
39,40	$\lambda_i$	C–Br	$Br_{10}-C_2-C_3-C_1, Br_{14}-C_6-C_5-C_1$
41	$\mu_i$	C–N	$N_7-C_1-C_2-C_6$
<b>Torsion</b>			
42 – 47	$\tau_i$	t Ring	$C_1-C_2-C_3-C_4, C_2-C_3-C_4-C_5,$ $C_3-C_4-C_5-C_6,$ $C_4-C_5-C_6-C_1, C_5-C_6-C_1-C_2,$ $C_6-C_1-C_2-C_3$
48	$\tau_i$	t C–NH <sub>2</sub>	$C_1-N_7-H_8-H_9$

<sup>a</sup>For numbering of atoms refer Fig. 1.

The vibrational analysis obtained for CDDBA with the unscaled HF and B3LYP/6-31+G(d,p) force field are generally somewhat greater than the experimental values due to neglect of anharmonicity in real system. These discrepancies can be corrected either by computing anharmonic corrections explicitly or by introducing a scaling the calculated wavenumbers with proper scale factor. Then, for an easier comparison to the observed values, the calculated frequencies are scaled to less than 1, to minimize the overall

deviation. Therefore, we have used the different scaling factor values of HF/6-31+G(d,p) methods. The results indicate that the B3LYP calculations approximate the observed fundamental frequencies much better than the HF results. Inclusion of electron correlation in density functional theory to a certain extent makes the frequency values smaller in comparison with HF frequency. Also, it should be noted that the experimental results belong to solid phase and theoretical calculations belong to gaseous phase. The resultant scaled frequencies are also listed in Table 6.

Table 3. Definition of local symmetry coordinates of 4-chloro-2,6-dibromoaniline

No. (i)	Type	Definition
1, 2	C H	$r_1, r_2$
3,4	C Br	$R_3, R_4$
5	C Cl	$q_5$
6	C N	$Q_6$
7 – 12	C C	$S_7, S_8, S_9, S_{10}, S_{11}, S_{12}$
13	NH <sub>2</sub> ss	$(P_{13} + P_{14}) / \sqrt{2}$
14	NH <sub>2</sub> ass	$(P_{13} - P_{14}) / \sqrt{2}$
15	Ring trigd	$(\alpha_{15} - \alpha_{16} + \alpha_{17} - \alpha_{18} + \alpha_{19} - \alpha_{20}) / \sqrt{6}$
16	Ring symd	$(-\alpha_{15} - \alpha_{16} + 2\alpha_{17} - \alpha_{18} - \alpha_{19} + 2\alpha_{20}) / \sqrt{12}$
17	Ring asymd	$(\alpha_{15} - \alpha_{16} + \alpha_{18} - \alpha_{19}) / 2$
18, 19	b C H	$(\beta_{21} - \beta_{22}) / \sqrt{2}, (\beta_{23} - \beta_{24}) / \sqrt{2}$
20	b C Cl	$(\nu_{25} - \nu_{26}) / \sqrt{2}$
21,22	b C Br	$(\sigma_{27} - \sigma_{28}) / \sqrt{2}, (\sigma_{29} - \sigma_{30}) / \sqrt{2}$
23	b C N	$(\delta_{31} - \delta_{32}) / \sqrt{2}$
24	NH <sub>2</sub> rock	$(\epsilon_{33} - \epsilon_{34}) / \sqrt{2}$
25	NH <sub>2</sub> twist	$(\epsilon_{33} + \epsilon_{34}) / \sqrt{2}$
26	NH <sub>2</sub> sciss	$(2\pi_{35} - \epsilon_{33} - \epsilon_{34}) / \sqrt{6}$
27, 28	$\omega$ C H	$\Psi_{36}, \Psi_{37}$
29	$\omega$ C Cl	$\omega_{38}$
30,31	$\omega$ C Br	$\lambda_{40}, \lambda_{40}$
32	$\omega$ C N	$\mu_{41}$
33	t Ring trigd	$(\tau_{42} - \tau_{43} + \tau_{44} - \tau_{45} + \tau_{46} - \tau_{47}) / \sqrt{6}$
34	t Ring symd	$(\tau_{42} - \tau_{44} + \tau_{45} - \tau_{47}) / \sqrt{2}$
35	t Ring asymd	$(-\tau_{42} + 2\tau_{43} - \tau_{44} - \tau_{45} + 2\tau_{46} - \tau_{47}) / \sqrt{12}$
36	t C–NH <sub>2</sub> wag	$\tau_{48}$

### C–H vibrations

The substituted benzene gives rise to C–H stretching, C–H in-plane bending and C–H out-of-plane bending deformation. The hetero aromatic structure shows the presence of C–H stretching vibrations in the region 3100 – 3000 cm<sup>-1</sup> which is the characteristic region for the ready identification of such C–H stretching vibrations [25]. Accordingly, in the present investigation, the C–H stretching vibrations of CDDBA is observed at 3082 cm<sup>-1</sup> in FTIR and 3083, 2989 cm<sup>-1</sup> in FT-Raman spectrum. The C–H in-plane and out-of-plane bending modes of CDDBA show consistent agreement with the computed B3LYP result and are listed in Table 6.

### C–C Vibrations

The C–C aromatic stretching vibrations gives rise to characteristic bands in the observed IR and Raman spectra, covering the spectral range from 1650 to 1400 cm<sup>-1</sup>.

**Table 4. The thermodynamic parameters of 4-chloro-2,6-di bromoaniline along with the global minimum energy calculated at HF/6-31+G(d,p) and B3LYP/6-31+G(d,p) methods**

Parameters	B3LYP/ 6-31+G(d,p)
Optimized global minimum energy (Hartrees)	-3777.8936
Zero-point vibrational energy(kcal mol <sup>-1</sup> )	55.70838
Rotational constants (GHz)	0.60186
	0.36872
	0.22867
Rotational temperature (Kelvin)	0.02888
	0.01770
	0.01097
Energy (kcal mol <sup>-1</sup> )	
Total	61.705
Translational	0.899
Rotational	0.889
Vibrational	59.927
Molar capacity at constant Volume (cal mol <sup>-1</sup> Kelvin)	
Total	34.507
Translational	2.9812
Rotational	2.9812
Vibrational	28.545
Entropy(cal mol <sup>-1</sup> Kelvin)	
Total	100.255
Translational	42.817
Rotational	33.115
Vibrational	24.322
Dipole moment(Debye)	
$\mu_x$	-1.8611
$\mu_y$	0.9750
$\mu_z$	2.1010
$\mu_{total}$	1.2149

Therefore, the C-C stretching vibrations of CDDBA are observed at 1561, 1463, 1445 cm<sup>-1</sup> in FTIR spectrum and 1611, 1575, 1467 cm<sup>-1</sup> in Raman. Most of the ring vibrational modes are affected by the substitutions in the aromatic ring of CDDBA [25]. The FTIR and Raman spectrum have been designated to ring in-plane bending modes by careful consideration of their quantitative descriptions. The ring out-of-plane bending modes of CDDBA are also listed in Table 6. The reductions in the frequencies to these modes are due to the change in force constant and the vibrations of the functional groups present in the molecule. The theoretically computed values for C-C vibrational modes by B3LYP/6-31+G(d,p) method gives excellent agreement with experimental data.

#### C-Cl vibrations

The vibrations belonging to the bond between the ring and the halogen atoms are worth to discuss here, since mixing of vibrations are possible due to the lowering of the molecule symmetry and the presence of heavy atoms on the periphery of molecule. Generally, the C-Cl absorption is obtained in the broad region between 850 – 550 cm<sup>-1</sup>. Therefore, the bands found at 702 cm<sup>-1</sup> in both IR, Raman have been assigned to C-Cl stretching vibrations of CDDBA and the corresponding force constant contribute nearly 75% to the TED. Most of the aromatic chloro compounds have the region 385 - 265 cm<sup>-1</sup> due to C-Cl in-plane bending vibration. Accordingly, the bands identified 625 cm<sup>-1</sup> in Raman is assigned to the C-Cl in-plane mode of CDDBA. The C-Cl out-of-plane deformation for the title compound has been established at 292 cm<sup>-1</sup> in the

Raman spectrum. These are in good agreement with the literature data [25].

#### C-Br vibrations

Strong characteristic absorption due to the C-Br stretching vibration is observed with the position of the bands being influenced by neighbouring.

The C-Br stretching vibrations given generally strong band in the region 1300-550 cm<sup>-1</sup> [25]. In the present investigation, the band observed at 1279 cm<sup>-1</sup> in FTIR spectrum and the bands observed at 1297, 1281 cm<sup>-1</sup> in FT-Raman spectrum are assigned to C-Br stretching vibration for CDDBA. The C-Br in-plane bending and out-of-plane bending vibration are assigned in the IR and Raman bands and are listed in Table 6.

#### NH<sub>2</sub> vibrations

The molecule under consideration posses NH<sub>2</sub> group and hence six internal modes of vibration are possible such as symmetric stretching, asymmetric stretching, scissoring, rocking, wagging and the torsional mode.

The NH<sub>2</sub> group has two (N-H) stretching vibrations; one being asymmetric and the other symmetric. The frequency of asymmetric vibration is higher than that of symmetric one. The frequencies of amino group in the region 3500 – 3300 cm<sup>-1</sup> for NH stretching, 1700 – 1600 for scissoring and 1150 – 900 for rocking deformation.

In the present investigation, the asymmetric and symmetric modes of NH<sub>2</sub> group in CDDBA are assigned at 3424 cm<sup>-1</sup> in IR and 3426 cm<sup>-1</sup> in Raman and 3302 cm<sup>-1</sup> in both IR, Raman spectra. The bands appeared at 1618 cm<sup>-1</sup> in FTIR for CDDBA have been assigned to scissoring mode of NH<sub>2</sub> group. The rocking, wagging, twisting deformation vibrations of NH<sub>2</sub> contribute to several normal modes in the low frequency region. The band observed at 1083 cm<sup>-1</sup> in Raman for CDDBA is assigned to NH<sub>2</sub> rocking vibrations, and the bands observed at 652 cm<sup>-1</sup> in both IR, Raman is assigned to CDDBA for NH<sub>2</sub> wagging modes of vibrations. The band observed at 194 cm<sup>-1</sup> in Raman is assigned to NH<sub>2</sub> twisting modes for CDDBA [25].

#### Vibrational contribution to NLO activity and first hyperpolarizability

The potential application of the CDDBA in the field of nonlinear optics demands the investigation of its structural and bonding features contributing to the hyperpolarizability enhancement, by analyzing the vibrational modes using IR and Raman spectroscopy. The ring stretching bands of CDDBA observed at 1561, 1463, 1445 cm<sup>-1</sup> in IR and have their counterparts in the Raman spectrum at 1611, 1575, 1467 cm<sup>-1</sup>, respectively and their relative intensities in IR and Raman spectrum are comparable. The first hyperpolarizability ( $\beta$ ) of this novel molecular system is calculated using the *ab-initio* HF method, based on the finite-field approach. In the presence of an applied electric field, the energy of a system is a function of the electric field. The first hyperpolarizability is a third-rank tensor that can be described by a 3 × 3 × 3 matrix. The 27 components of the 3D matrix can be reduced to 10 components due to the Kleinman symmetry [26]. The components of  $\beta$  are defined as the coefficients in the Taylor series expansion of the energy in the external electric field.

**Table 5. The observed (FTIR and FT-Raman) and calculated (unscaled and scaled) frequencies ( $\text{cm}^{-1}$ ), IR intensity ( $\text{km mol}^{-1}$ ), Raman activity ( $\text{\AA} \text{amu}^{-1}$ ) and force constant (m dyne  $\text{\AA}$ ) and probable assignments (Characterized by TED) of 4-chloro-2,6-dibromoaniline using HF/6-31+G(d,p) and B3LYP /6-31+G(d,p) calculations**

Symmetry species $C_s$	Observed frequencies ( $\text{cm}^{-1}$ )		Calculated frequencies ( $\text{cm}^{-1}$ ) (Unscaled)		Scaling frequency ( $\text{cm}^{-1}$ )		Force constant (mDyne/ $\text{\AA}$ )		IR intensity (KM/Mole)		Raman activity ( $\text{\AA}^4/\text{amu}$ )		Assignments (% TED)
	FTIR	FT-Raman	HF	B3LYP	HF	B3LYP	HF	B3LYP	HF	B3LYP	HF	B3LYP	
A'	3424(vw)	3426(vw)	3838	3567	3475	3426	9.4976	8.1864	21.267	9.1078	67.0655	75.880	NH <sub>2</sub> ass(98)
A'	3302(w)	3302(s)	3751	3494	3415	3305	8.7006	7.5442	20.670	10.091	134.818	174.755	NH <sub>2</sub> ss (96)
A'	3082(w)	3083(w)	3409	3243	3295	3085	7.4968	6.7725	1.0994	1.2436	47.2532	58.395	vCH (94)
A'	-	2989(vw)	3408	3242	3100	2993	7.4954	6.7678	1.1080	1.4976	55.4449	50.657	vCH (95)
A'	1618(s)	-	1999	1761	1692	1623	2.4286	1.9766	59.776	5.0985	15.4177	23.0789	NH <sub>2</sub> sciss (89), vCH (12)
A'	-	1611(s)	1876	1717	1657	1615	12.641	10.787	43.455	5.7521	23.3909	34.8064	vCC (72), vCH (15)
A'	-	1575(s)	1786	1680	1610	1579	7.2203	8.0475	29.268	37.286	5.9647	9.5880	vCC (84), vCH (21)
A'	1561(s)	-	1698	1581	1596	1564	5.8036	4.7543	121.52	11.849	1.2445	2.5875	vCC (69) vCBr (23)
A'	-	1467(w)	1632	1510	1510	1469	4.0490	3.6181	51.560	51.718	0.2633	0.2056	vCC (60), vCBr(26)
A'	1463(w)	-	1595	1512	1494	1466	3.2226	7.8744	9.3403	2.4514	7.6582	3.7067	vCC (65), NH <sub>2</sub> sciss(19)
A'	1445(vw)	-	1553	1509	1485	1448	1.7524	3.0865	10.070	9.3512	0.5749	13.2785	vCC (64), bCH (14)
A'	-	1297(s)	1523	1498	1380	1299	4.6308	1.3966	2.1910	0.054	0.8151	0.1562	vCBr(62), vCC (120)
A'	1279(w)	1281(vw)	1478	1339	1316	1286	2.1912	2.5799	4.6894	3.5252	10.1109	7.1999	vCBr (61), vCC (13)
A'	1215(vw)	-	1320	1240	1231	1228	6.6863	2.1858	0.3574	4.0323	2.6087	6.7369	bCH (60)
A'	-	1127(w)	1297	1230	1214	1135	1.0309	0.7562	247.31	219.18	0.8836	3.7468	bCH (61)
A'	-	1083(w)	1260	1208	1194	1089	3.4440	2.7904	17.298	13.603	22.5456	19.6156	NH <sub>2</sub> rock(56), vCC(26), vCBr(11)
A'	1075(w)	-	1245	1188	1156	1087	1.2657	1.4827	37.355	38.057	0.8134	0.6970	Rasymd(60), vCC (25), vCBr(12)
A'	930(w)	-	1159	1009	985	939	2.8838	2.6290	46.465	53.041	5.3795	6.8150	Rsymd (65), vCC(23), bCCl (11)
A'	784(w)	-	1001	962	895	790	0.9499	0.8341	10.183	9.3156	2.4218	2.0610	Rtrigd60, vCCl(21), tRasymd(19)
A'	-	752(vw)	988	949	845	759	1.0436	0.8853	3.2314	4.1779	2.8383	2.0384	vCN(62), bCH (23), tRsymd (12)
A'	702(vw)	702(w)	946	883	813	709	1.4649	1.2623	1.4004	2.2484	6.6862	5.7226	vCCl(61), bCH(15), t R trigd (10)
A'	652(w)	652(vw)	848	792	762	700	0.2986	0.2589	5.4187	5.4445	0.1453	0.1952	NH <sub>2</sub> wag(68), v CN (16)
A'	-	625(vs)	804	698	670	632	0.8354	0.7213	0.9580	1.1966	8.6436	7.0384	bCCl (69), bCN (17)
A'	621(vw)	-	796	630	658	629	0.8844	0.7556	0.0152	0.0011	2.8452	2.9837	bCBr(66), R asymd (11)
A'	-	541(s)	660	598	566	548	0.3301	0.2334	0.0946	0.0488	2.0493	2.4264	bCBr (65), R symd (12)
A''	535(s)	-	653	623	619	545	1.3345	1.1135	0.0026	0.1515	0.7954	1.3919	bCN (67), R trigd (14)
A''	-	531(s)	621	611	593	539	0.8626	0.6553	0.9238	4.1887	0.6050	1.0925	$\omega$ CH (62), bCBr(10)
A''	-	441(vw)	550	534	495	451	0.9212	0.6645	28.389	22.073	0.2143	0.4013	$\omega$ CH (60), bCBr(16)
A''	-	408(vw)	520	501	478	419	1.3276	1.1802	7.1191	2.8102	0.6511	0.3511	t R asymd (59)
A''	-	398(vw)	501	473	452	407	0.9832	0.8468	4.4987	3.6346	0.3292	0.5782	t R symd (58)
A''	394(vw)	-	490	467	430	399	1.0935	0.8857	0.0011	0.0187	0.3228	0.8013	t R trigd (60)
A''	390(vw)	-	478	428	421	397	0.3900	0.3575	0.7360	0.8230	1.8617	1.3618	$\omega$ CN (56)
A''	-	377(s)	463	409	389	385	0.1413	0.1186	0.3516	0.3781	1.5372	1.5255	$\omega$ CBr (55)
A''	-	292(vw)	430	387	370	298	0.1323	0.1117	0.4338	0.2561	0.2444	0.2946	$\omega$ CCl (53)
A''	-	224(w)	410	337	265	229	0.0375	0.0323	0.7239	0.6879	0.2663	0.3635	$\omega$ CBr (54)
A''	-	194(w)	310	270	247	202	0.0380	0.0551	52.132	51.465	2.2101	2.3505	NH <sub>2</sub> twist (52)

Abbreviations: v - stretching; b - in-plane bending;  $\omega$  - out-of-plane bending; asymd - asymmetric; symd - symmetric; t - torsion; trig - trigonal; w - weak; vw - very weak; vs - very strong; s - strong; ms - medium strong; ss - symmetric stretching; ass - asymmetric stretching; ips - in-plane stretching; ops - out-of-plane stretching; sb - symmetric bending; ipr - in-plane rocking; opr - out-of-plane rocking; opb - out-of-plane bending.

When the electric field is weak and homogeneous, this expansion becomes

$$E = E_0 - \sum_i \mu_i F^i - \frac{1}{2} \sum_{ij} \alpha_{ij} F^i F^j - \frac{1}{6} \sum_{ijk} \beta_{ijk} F^i F^j F^k - \frac{1}{24} \sum_{ijkl} \nu_{ijkl} F^i F^j F^k F^l$$

where  $E_0$  is the energy of the unperturbed molecule;  $F^i$  is the field at the origin; and  $\mu_i$ ,  $\alpha_{ij}$ ,  $\beta_{ijk}$  and  $\nu_{ijkl}$  are the components of dipole moment, polarizability, the first hyper polarizabilities and second hyperpolarizabilities, respectively. The total static dipole moment  $\mu$ , the mean polarizability  $\alpha_0$  and the mean first hyperpolarizability  $\beta_0$ , using the  $x$ ,  $y$ ,  $z$  components they are defined as:

$$\mu = (\mu_x^2 + \mu_y^2 + \mu_z^2)^{1/2}$$

$$\alpha_0 = \frac{(\alpha_{xx} + \alpha_{yy} + \alpha_{zz})}{3}$$

$$\alpha = 2^{-1/2} \left[ (\alpha_{xx} - \alpha_{yy})^2 + (\alpha_{yy} - \alpha_{zz})^2 + (\alpha_{zz} - \alpha_{xx})^2 + 6\alpha_{xy}^2 \right]^{1/2}$$

$$\beta_0 = (\beta_x^2 + \beta_y^2 + \beta_z^2)^{1/2}$$

and

$$\beta_x = \beta_{xxx} + \beta_{xyy} + \beta_{xzz}$$

$$\beta_y = \beta_{yyy} + \beta_{xyx} + \beta_{yzz}$$

$$\beta_z = \beta_{zzz} + \beta_{xxz} + \beta_{yyz}$$

**Table 6.** Calculated atomic charges of 4-chloro-2,6-dibromoaniline by natural bond orbital (NBO) analysis by B3LYP method

Atom No	Charge	Core	Valence	Total
C1	0.09747	1.99858	3.88356	5.90253
C2	-0.12760	1.99849	4.10716	6.12760
C3	-0.25366	1.99884	4.23812	6.25366
C4	-0.04911	1.99859	4.02798	6.04911
C5	-0.25013	1.99884	4.23471	6.25013
C6	-0.11705	1.99850	4.09500	6.11705
N7	-0.89477	1.99962	5.87333	7.89477
H8	0.41380	0.00000	0.58380	0.58620
H9	0.40975	0.00000	0.58739	0.59025
Br10	0.09150	27.99873	6.89097	34.90850
H11	0.27244	0.00000	0.72534	0.72756
Cl12	0.02242	9.99966	6.95810	16.97758
H13	0.27427	0.00000	0.72346	0.72573
Br14	0.11067	27.99874	6.87230	5.0825

The calculated mean first hyperpolarizability ( $\beta$ ) of the title compounds CDBA are  $0.953 \times 10^{-30}$  esu, respectively, which are comparable with the reported values of similar derivatives [26]. The large value of hyperpolarizability  $\beta$  which is a measure of the non-linear optical activity of the molecular system is associated with the intermolecular charge transfer, resulting from the electron cloud movement through  $\pi$  conjugated frame work from electron donor to electron acceptor groups. The physical properties of these conjugated molecules are governed by the high gaps. So, we conclude that the title compounds are an attractive object for future studies of nonlinear optical properties.

#### Homo-Lumo Analysis

Many organic molecule, containing conjugated  $\pi$  electrons are characterized by large values of molecular first

hyper polarizabilities, and they are analyzed by means of vibrational spectroscopy [27]. In most of the cases, even in the absence of inversion symmetry, the strongest band in the Raman spectrum is weak in the IR spectrum and vice-versa. But the intramolecular charge from the donor to acceptor group through a single-double bond conjugated path can induce large variations of both the molecular dipole moment and the molecular polarizability, making IR and Raman activity strong at the same time. The experimental spectroscopic behaviour described above is well accounted for DFT calculations in  $\pi$  conjugated system that predict exceptionally infrared intensities for the same normal modes. The analysis of the wave function indicates that the electron absorption corresponds to the transition from the ground to the first excited state and is mainly described by one-electron excitation from the highest occupied molecular orbital (HOMO) to the lowest unoccupied orbital (LUMO). The LUMO; of  $\pi$  nature, (i.e. benzene ring) is delocalized over the whole C-C bond.

By contrast, the HOMO is located over  $\text{NH}_2$  atoms; consequently the HOMO  $\rightarrow$  LUMO transition implies an electron density transfer to aromatic part and  $\text{NH}_2$  of  $\pi$  conjugated system from benzene ring. Moreover, these three orbital's significantly overlap in the Para position of the benzene ring for CDBA. The atomic orbital compositions of the frontier molecular orbital are shown in Fig. 4.

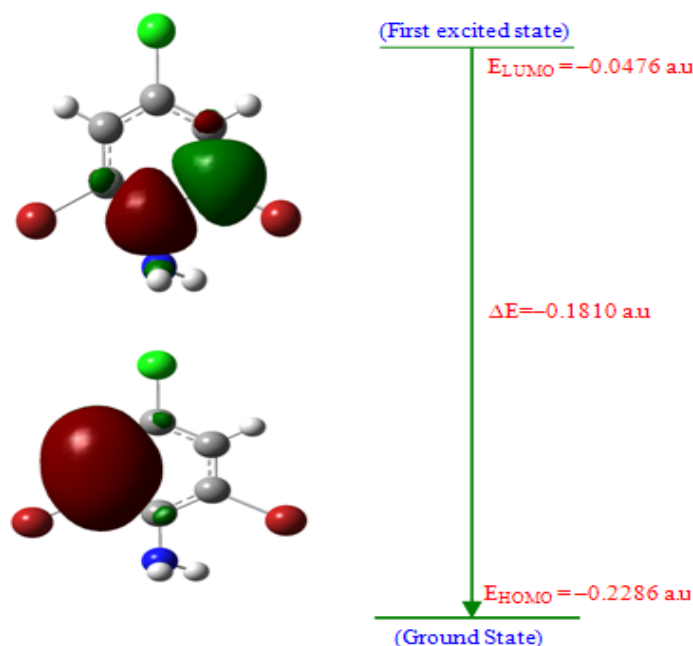


**Fig 4.** HOMO-LUMO of 4-chloro-2,6-dibromoaniline

The HOMO $\rightarrow$ LUMO energy gap of CDBA is calculated using HF/6-31+G(d,p) and B3LYP/6-31+G(d,p) level, reveals that the energy gap reflects the chemical activity of the molecules. The LUMO as an electron acceptor (EA) represents the ability to obtain an electron (ED), and HOMO represents the ability to donate an electron (ED). The ED groups to the efficient EA groups through  $\pi$ -conjugated path. The strong charge transfer interaction through  $\pi$ -conjugated bridge results insubstantial ground state donor-Acceptor (DA) mixing and the appearance of a charge transfer band in the electron absorption spectrum. For CDBA,

Table 7. The atomic orbital occupancies of 4-chloro-2,6-dibromoaniline

Atom No	Atomic orbital	Type	Occupancy	Energy
C1	1s	Core	0.99929	-10.11615
	2s	Valence	0.42991	-0.19173
	2p <sub>x</sub>	Valence	0.54490	-0.10123
	2p <sub>y</sub>	Valence	0.46523	-0.09244
	2p <sub>z</sub>	Valence	0.50175	-0.14579
C2	1s	Core	0.99925	-10.14082
	2s	Valence	0.47942	-0.26739
	2p <sub>x</sub>	Valence	0.50015	-0.17565
	2p <sub>y</sub>	Valence	0.53112	-0.13400
	2p <sub>z</sub>	Valence	0.54289	-0.17418
C3	1s	Core	0.99942	-10.07779
	2s	Valence	0.47918	-0.21339
	2p <sub>x</sub>	Valence	0.59125	-0.10523
	2p <sub>y</sub>	Valence	0.54782	-0.09490
	2p <sub>z</sub>	Valence	0.50081	-0.14384
C4	1s	Core	0.99930	-10.15001
	2s	Valence	0.47024	-0.26109
	2p <sub>x</sub>	Valence	0.54358	-0.10588
	2p <sub>y</sub>	Valence	0.46447	-0.17872
	2p <sub>z</sub>	Valence	0.53570	-0.16876
C5	1s	Core	0.99942	-10.07650
	2s	Valence	0.47989	-0.21222
	2p <sub>x</sub>	Valence	0.59253	-0.10361
	2p <sub>y</sub>	Valence	0.54662	-0.09270
	2p <sub>z</sub>	Valence	0.49831	-0.14200
C6	1s	Core	0.99925	-10.13773
	2s	Valence	0.47974	-0.26322
	2p <sub>x</sub>	Valence	0.50441	-0.16927
	2p <sub>y</sub>	Valence	0.52918	-0.12804
	2p <sub>z</sub>	Valence	0.53417	-0.16828
N7	1s	Core	0.99981	-14.19507
	2s	Valence	0.70664	-0.58062
	2p <sub>x</sub>	Valence	0.85110	-0.24053
	2p <sub>y</sub>	Valence	0.63738	-0.20406
	2p <sub>z</sub>	Valence	0.74154	-0.21898
H8	1s	Valence	0.29190	0.13661
H9	1s	Valence	0.29370	0.13965
Br10	1s	Core	1.00000	-476.35301
	2s	Core	0.99996	-61.65895
	3s	Core	0.99974	-15.11904
	4s	Valence	0.93438	-1.03936
	2p <sub>x</sub>	Core	0.99998	-55.46011
	3p <sub>x</sub>	Core	0.99994	-7.53218
	4p <sub>x</sub>	Valence	0.66108	0.28076
	2p <sub>y</sub>	Core	0.99999	-55.45820
	3p <sub>y</sub>	Core	0.99997	-7.52701
	4p <sub>y</sub>	Valence	0.88345	-0.30905
Br14	1s	Core	1.00000	-100.17221
	2s	Core	0.99989	-10.57899
	3s	Valence	0.92059	-1.01104
	2p <sub>x</sub>	Core	0.99999	-1.01104
	3p <sub>x</sub>	Valence	0.98461	-0.33768
	2p <sub>y</sub>	Core	0.99995	-7.24518
	3p <sub>y</sub>	Valence	0.60881	-0.28615
	2p <sub>z</sub>	Core	1.00000	-7.23720
	3p <sub>z</sub>	Valence	0.96504	-0.33602
	H11	1s	Valence	0.36267
Br14	1s	Core	1.00000	-476.34441
	2s	Core	0.99996	-61.66163
	3s	Core	0.99974	-15.08715
	4s	Valence	0.93454	-1.01899
	2p <sub>x</sub>	Core	0.99998	-55.44435
	3p <sub>x</sub>	Core	0.99994	-7.51947
	4p <sub>x</sub>	Valence	0.65868	-0.26512
	2p <sub>y</sub>	Core	0.99999	-55.44237
	3p <sub>y</sub>	Core	0.99997	-7.51408
	4p <sub>y</sub>	Valence	0.87885	-0.29097
H13	1s	Valence	0.36173	0.08091
	2p <sub>z</sub>	Core	1.00000	-55.44173
	3p <sub>z</sub>	Core	0.99999	-7.51247
	4p <sub>z</sub>	Valence	0.96408	-0.30562

The HOMO-LUMO energy gap explains the fact that eventual charge transfer interaction is taking place within the molecule.

	HF	B3LYP
HOMO energy	-0.3170 a.u	-0.2286 a.u
LUMO energy	-0.0472 a.u	-0.0476 a.u
Energy gap( $\Delta E$ )	-0.2698 a.u	-0.1810 a.u

#### Natural Bond Orbital Analysis

Natural bond orbital (NBO) methods encompass a suite of algorithms that enable fundamental bonding concepts to be extracted from Hartree-Fock (HF), Density Functional Theory (DFT) and post-HF computations.

NBO analysis originated as a technique for studying hybridisation and covalency effects in polyatomic wave functions, based on local block eigen vectors of the one-particle density matrix. NBOs would correspond closely to the picture of localised bonds and lone pairs as basic units of molecular structure. The atomic charges, core, valences and total charge of CDBA calculated by NBO analysis using the B3LYP/6-31+G(d,p) method are presented in Table 6. Among the ring carbon atoms C2 and C6 for CDBA have same negative charges. But N7 has more negative charge due to the resonance of amino group for CDBA. The both charges of H8 for CDBA are same. In Table 7, the natural atomic orbitals, their occupancies and the corresponding energy of CDBA are described. In a given molecular environment the natural atomic orbitals reflect the chemical give and take of electronic interactions, with variations of shape (e.g., angular deformations due to steric pressures of adjacent atoms) and size (e.g., altered diffuseness due to increased 250 anionic or cationic characters) that distinguish them appreciably for free atom forms. The NAOs orbital energies  $\epsilon_i$  (A) are calculated by using Kohn-Sham operator ( $F$ ) as

$$\epsilon_i^{(A)} = \langle \theta_i^{(A)} | F | \theta_i^{(A)*} \rangle$$

The NAOs deals the molecular properties in terms of inter atomic and intra atomic contributions. The Table 8 depicts the bonding concepts such as type of bond orbital, their occupancies, the natural atomic hybrids of which the NBO is composed, giving the percentage of the NBO on each hybrid, the atom label, and a hybrid label showing the hybrid orbital ( $sp^x$ ) composition (the amount of  $s$ -character,  $p$ -character, etc.), of CDBA molecule determined by B3LYP/6-31+G(d,p) method with respectable accuracy. The lone pair orbital structure of  $sp^2$  is represented in Fig. 5 for CDBA.

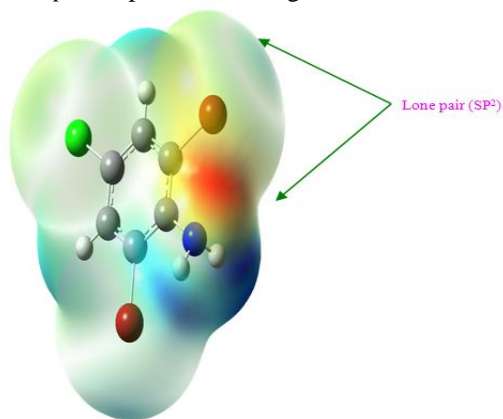


**Fig 5. The lone pair structure of 4-chloro-2,6-dibromoaniline**

The occupancies of NBOs in CDBA reflect their exquisite dependence on the chemical environment. The NBO energy values show the corresponding spatial symmetry breaking in

the direction of unpaired spin. The Lewis structure that is closest to the optimised structure is determined. The hybridisation of the atoms and the weight of each atom in each localised electron pair bond is calculated in this idealised Lewis structure and presented in Table 8.

**Table 8. Bond orbital analysis of 4-chloro-2,6-dibromoaniline by B3LYP/ 6-31+G(d,p) method**

Bond orbital	Occupancy	Atom	Contribution from parent NBO (%)	Coefficients	Atom Hybrid Contributions (%)
C1-C2	0.98717	C1	50.02	0.7073	s(36.22) + p 1.76(63.73)
		C2	49.98	0.7069	s(38.10) + p 1.62(61.86)
C1-C6	0.98613	C1	50.36	0.7096	s(36.49) + p 1.74(63.47)
		C6	49.64	0.7046	s(37.83) + p 1.64(62.13)
C1-N7	0.99447	C1	42.92	0.6551	s(27.10) + p 2.69(72.82)
		N7	57.08	0.7555	s(28.90) + p 2.46(71.03)
C2-C3	0.98700	C2	50.77	0.7126	s(38.76) + p 1.58(61.20)
		C3	49.23	0.7016	s(34.53) + p 1.89(65.43)
C2-Br10	0.99215	C2	49.91	0.7064	s(23.14) + p 3.32(76.76)
		Br10	50.09	0.7078	s(12.97) + p 6.69(86.75)
C3-C4	0.98721	C3	49.49	0.7035	s(34.51) + p 1.90(65.45)
		C4	50.51	0.7107	s(37.99) + p 1.63(61.97)
C3-H11	0.98948	C3	63.72	0.7983	s(30.92) + p 2.23(69.04)
		H11	36.28	0.6023	s(99.94) + p 0.00(0.06)
C4-C5	0.98748	C4	50.60	0.7113	s(38.07) + p 1.63(61.89)
		C5	49.40	0.7028	s(34.37) + p 1.91(65.59)
C4-Cl12	0.99458	C4	46.36	0.6809	s(23.90) + p 3.18(75.94)
		Cl12	53.64	0.7324	s(16.74) + p 4.95(82.78)
C5-C6	0.98702	C5	49.34	0.7024	s(34.57) + p 1.89(65.39)
		C6	50.66	0.7118	s(38.63) + p 1.59(61.33)
C5-H13	0.98940	C5	63.81	0.7988	s(31.02) + p 2.22(68.95)
		H13	36.19	0.6016	s(99.94) + p 0.00(0.06)
C6-Br14	0.99166	C6	50.80	0.7127	s(23.54) + p 3.24(76.37)
		Br14	49.20	0.7014	s(12.75) + p 6.82(86.97)
N7-H8	0.98905	N7	70.69	0.8408	s(25.47) + p 2.92(74.47)
		H 8	29.31	0.5414	s(99.89) + p 0.00(0.11)
N7-H 9	0.99397	N7	70.86	0.8418	s(28.17) + p 2.55(71.76)
		H9	29.14	0.5398	s(99.89) + p 0.00(0.11)

For CDBA, no antibonding orbitals are listed so that the structure is adequately explained by normal Lewis electron pair orbitals. For example, the bonding orbital for C1-N7 with 0.99447 electrons has 42.92% C1 character in a  $sp$  2.69 hybrid and has 57.08% N7 character in a  $sp$  2.46 hybrid orbital of CDBA. The bonding orbital C2-Br10 with 0.99215 electrons has 49.91% C2 character in a  $sp$  3.32 hybrid and has 50.09% Br 10 character in a  $sp$  6.69 hybrid orbital for CDBA. A bonding orbital for C4-Cl12 with 0.99458 electrons has 46.36 % C4 character in a  $sp$  3.18 hybrid and has 53.64% Cl12 character in a  $sp$  4.95 hybridised orbital for CDBA [28].

### Donor Acceptor Interactions: Perturbation Theory Energy Analysis

The localised orbitals in the Lewis structure of CDBA can interact strongly. A filled bonding or lone pair orbital can act as a donor and an empty or filled bonding, antibonding, or lone pair orbital can act as an acceptor. These interactions can strengthen and weaken bonds. For example, lone pair donor  $\rightarrow$  antibonding acceptors orbital interaction may 251 weaken the bond associated with the antibonding orbital. Conversely, an interaction with a bonding pair as the acceptor may strengthen the bond. Strong electron delocalisation in the Lewis structure also shows up as donor-acceptor interactions. The stabilisation energy of different kinds of interactions are listed Table 9.

**Table 9. Second order perturbation theory analysis of Fock matrix of 4-chloro-2,6-dibromoaniline by NBO method**

Donor (i) $\rightarrow$ Acceptor (j)	$E^{(2)a}$ (kJ mol <sup>-1</sup> )	$E(j) - E(i)^b$ (a.u.)	$F(i, j)^c$ (a.u.)
$\sigma C1-C2 \rightarrow \sigma^* C1-C6$	7.78224	1.28	0.062
$\sigma C1-C2 \rightarrow \sigma^* C6-Br14$	8.07512	0.83	0.050
$\pi C1-C2 \rightarrow \pi^* C3-C4$	43.42992	0.28	0.069
$\pi C1-C2 \rightarrow \pi^* C5-C6$	35.31296	0.28	0.063
$\sigma C1-C6 \rightarrow \pi^* C1-C2$	7.61488	1.28	0.061
$\sigma C1-C6 \rightarrow \sigma^* C2-Br10$	8.45168	0.81	0.051
$\sigma C2-C3 \rightarrow \sigma^* C4-Cl12$	8.28432	0.87	0.052
$\sigma C3-C4 \rightarrow \sigma^* C2-Br10$	9.16296	0.80	0.053
$\pi C3-C4 \rightarrow \pi^* C1-C2$	35.85688	0.28	0.063
$\pi C3-C4 \rightarrow \pi^* C5-C6$	43.01152	0.28	0.069
$\sigma C4-C5 \rightarrow \sigma^* C6-Br14$	8.82824	0.81	0.052
$\sigma C5-C6 \rightarrow \sigma^* C1-N7$	7.9496	1.07	0.057
$\sigma C5-C6 \rightarrow \sigma^* C4-Cl12$	8.40984	0.86	0.053
$\pi C5-C6 \rightarrow \pi^* C1-C2$	45.22904	0.27	0.070
$\pi C5-C6 \rightarrow \pi^* C3-C4$	36.8192	0.28	0.063
$n_1 N7 \rightarrow \sigma^* C1-C2$	13.22144	0.84	0.066
$n_1 N7 \rightarrow \pi^* C1-C2$	9.37216	0.30	0.036
$n_2 N7 \rightarrow \sigma^* C1-C6$	4.26768	0.84	0.037
$n_1 Br10 \rightarrow \sigma^* C1-C2$	6.86176	0.84	0.047
$n_2 Br10 \rightarrow \sigma^* C2-C3$	6.4852	0.84	0.046
$n_1 Br10 \rightarrow \pi^* C1-C2$	20.7108	0.30	0.054
$n_1 Cl 12 \rightarrow \sigma^* C3-C4$	8.61904	0.86	0.053
$n_1 Cl 12 \rightarrow \pi^* C3-C4$	25.68976	0.32	0.061

<sup>a</sup> $E^{(2)}$  means energy of hyperconjugative interactions (stabilization energy).

<sup>b</sup>Energy difference between donor and acceptor i and j NBO orbitals.

<sup>c</sup> $F(i, j)$  is the Fock matrix element between i and j NBO orbitals.

This calculation is done by examining all possible interactions between 'filled' (donor) Lewis-type NBOs and 'empty' (acceptor) non-Lewis NBOs, and estimating their energetic importance by 2<sup>nd</sup> order perturbation theory. Since these interactions lead to loss of occupancy from the localised NBOs of the idealised Lewis structure into the empty non-Lewis orbitals (and thus, to departures from the idealised Lewis structure description), and they are referred to as 'delocalisation' corrections to the natural Lewis structure.

The NBO method demonstrates the bonding concepts like atomic charge, Lewis structure, bond type, hybridization, bond order, charge transfer and resonance weights. Natural bond orbital (NBO) analysis is a useful tool for understanding delocalisation of electron density from occupied Lewis-type (donor) NBOs to properly unoccupied non-Lewis type (acceptor) NBOs within the molecule. The stabilisation of

orbital interaction is proportional to the energy difference between interacting orbitals. Therefore, the interaction having strongest stabilisation takes place between effective donors and effective acceptors. This bonding-anti bonding interaction can be quantitatively described in terms of the NBO approach that is expressed by means of second-order perturbation interaction energy  $E^{(2)}$  [28]. This energy represents the estimate of the off-diagonal NBO Fock matrix element. The stabilisation energy  $E^{(2)}$  associated with  $i$  (donor)  $\rightarrow j$  (acceptor) delocalisation is estimated from the second-order perturbation approach as given below.

$$E^{(2)} = DE_{ij} = q_i \frac{F(i, j)^2}{\epsilon_j - \epsilon_i}$$

where,  $q_i$  is the donor orbital occupancy,  $\epsilon_i$  and  $\epsilon_j$  are diagonal elements (orbital energies) and  $F(i, j)$  is the off-diagonal Fock matrix element. In the bond pair donor orbital,  $\sigma CC \rightarrow \pi^* CC$  interaction between the C1-C6 bond pair and the antiperiplanar C1-C2 antibonding orbital give stabilisation of 7.61488 kJ mol<sup>-1</sup> for CDBA. The bond pair donor orbital,  $\sigma CC \rightarrow \sigma^* CC$  interaction between the C5-C6 bond pair and the antiperiplanar C1-N7 antibonding orbital gives stabilisation of 7.9496 kJ mol<sup>-1</sup> for CDBA. The 252 lone pair donor orbital,  $nBr \rightarrow \pi^* CC$  interaction between the Br10 carbon lone pair and the antiperiplanar C1-C2 antibonding orbital is seen to give a strong stabilisation, 20.7108 kJ mol<sup>-1</sup> for CDBA. The lone pair donor orbital,  $nN \rightarrow \sigma^* CC$  interaction between the N7 lone pair and the antiperiplanar C1-C2 antibonding orbital is seen to give a strong stabilisation, 13.22144 kJ mol<sup>-1</sup> for CDBA. The Fig. 5 shows that local negative electrostatic potentials (red) signal for C atoms with lone pairs whereas local positive electrostatic potentials (blue) signal for NH<sub>2</sub> atoms for CDBA.

### Conclusion

The molecular structural parameters, thermodynamic properties and fundamental vibrational frequencies of the optimized geometry of CDBA, have been obtained from *ab initio* HF and DFT calculations. The theoretical results are compared with the experimental results. Although both types of calculations are useful to explain vibrational spectra of CDBA, *ab initio* calculations at HF/6-31+G(d,p) level, it is found a little poorer than DFT/ B3LYP/6-31+G(d,p) level calculations. On the basis of agreement between the calculated experimental results, assignments of all the fundamental vibrational modes of CDBA have been made for the first time in this investigation. The TED calculation regarding the normal modes of vibration provided a strong support for the frequency assignment. Therefore, the assignments proposed at higher level of the theory with higher basis set with only reasonable deviation from the experimental values seems to be correct. Furthermore, the thermodynamic, nonlinear optical, first-order hyperpolarizabilities and total dipole moment properties of the compounds have been calculated in order to get insight into the compound. And also HOMO and LUMO energy gap explains the eventual charge transfer interaction taking place within the molecules. The NBO analysis has been performed in order to elucidate charge transfers or conjugative interaction, the intra-molecule rehybridization and delocalization of electron density within the molecule and bond pair donor orbital,  $\pi CC \rightarrow \pi^* CC$  interaction between the C1-C2 bond pair and the C3-C4 antibonding orbital give more stabilisation of 43.4299 kJ mol<sup>-1</sup> for CDBA

**Reference**

- [1] F.A. Diaz, C.O. Sanchez, M.A. Del Valle, J.I. Torres, L.H. Tagle, *Synth. Met.*, 118 (2001) 25.
- [2] S.C. Ng, L. Xu, *Adv. Matter*, 10 (1998) 1525.
- [3] R.A. Misra, S. Dubey, B.M. Prasad, D. Singh, *Indian J. Chem, sect A*, 38 (1999) 141.
- [4] V. Prevost, A. Petit, F. Pla, *Synth. Met.*, 104 (1999) 79.
- [5] M. Kanungo, A. Kumar, A.Q. Contractors, *Electroanal J. Chem.*, 528 (2002) 46.
- [6] Y. Dong, Mu, *Electrochem Acta* 36 (1991) 2015.
- [7] D.M. Delong champ, P.T. Hammond, *Chem. Mater*, 16 (2004) 4799.
- [8] R.G. Parr, W. Yang, *Density Functional Theory of Atoms and Molecules*, Oxford University Press, New York, 1989.
- [9] P. Pulay, G. Fogarasi, X. Zhou, P.W. Taylor, *Vib. Spectrosc.*, 1 (1990) 159.
- [10] H.A. Kramers, W. Heisenberg, *J. Phys.* 31 (1925) 681.
- [11] J.M.L. Martin, C.V. Alsenoy, *J. Phys. Chem.* 100 (1996) 6973.
- [12] J.M.L. Martin, J.E.I. Yazal, J.P. Francis, *J. Phys. Chem.* 100 (1996) 15358.
- [13] M.J. Frisch, G.W. Trucks, H.B. Schlegel, *GAUSSIAN 09*, Revision A.02, Gaussian, Inc., Wallingford, CT, 2009.
- [14] C. Lee, W. Yang, R. G. Parr, *Phys. Rev.* B37 (1988) 785.
- [15] T. Sundius, *J. Mol. Struct.*, 218 (1990) 321.
- [16] T. Sundius, *Vib. Spectrosc.*, 29 (2002) 89.
- [17] MOLVIB (V.7.0): Calculation of Harmonic Force Fields and Vibrational Modes of Molecules, QCPE Program No. 807 (2002).
- [18] A. Frisch, A.B. Nielson, A.J. Holder, *Gaussview User Manual*, Gaussian Inc., Pittsburg, PA, 2000.
- [19] P.L. Polavarapu, *J. Phys. Chem.* 94 (1990) 8106.
- [20] G. Keresztury, *Raman spectroscopy theory*, in: JM Chalmers, P. R. Griffiths (Eds.), *Handbook of Vibrational Spectroscopy*, Vol. 1, John Wiley & Sons Ltd., 2002, p. 71.
- [21] G. Keresztury, S. Holly, J. Varga, G. Besenyei, A.Y. Wang, J.R. Durig, *Spectrochim Acta part 49A* (1993) 2007.
- [22] M. Fukuyo, K. Hirotsu, T. Higuchi, *Acta Cryst.* 38B, (1982) 640.
- [23] M. Gdaniec *Acta Cryst.* E63, o2954.
- [24] G. Fogarasi, P. Ulay, in: J.R. Durig (Ed.) *Vibrational Spectra and Structure*, Vol.14, Elsevier, Amsterdam, 1985, P. 125, Chapter 3.
- [25] K. Sambathkumar, *Density Functional Theory Studies of Vibrational Spectra, Homo- Lumo, Nbo and Nlo Analysis of Some Cyclic and Heterocyclic Compounds* (Ph.D. thesis), Bharathidasan University, Tiruchirappalli, August 2014.
- [26] K. Sambathkumar, S. Jeyavijayan, M. Arivazhagan *Spectrochim Acta A* 147 (2015)51-66.
- [27] *D.Cecily Mary Glory*, R. Madivanane and K. Sambathkumar *Elixir Comp. Chem.* 89 (2015) 36730-36741.
- [28] Kuppusamy Sambathkumar *Spectrochim. Acta A* 147 (2015) 51-66.
- [29] M. Gdaniec *Acta Cryst.* E63, o2954.